COMMENT

Comment on "Nature of the Seismic Lithosphere-Asthenosphere Boundary within Normal Oceanic Mantle from High-Resolution Receiver Functions" by Olugboji et al.

Hitoshi Kawakatsu[1] and Yuki Abe[1,2]

[1]Earthquake Research Institute, The University of Tokyo, Tokyo, Japan, [2]Hot Springs Research Institute of Kanagawa Prefecture, Odawara, Japan

Key Points:
- Sediment reverberations are significant and severe for some of OBS data analyzed by *Olugboji et al.* [2016, G-cubed]
- Without considering this effect, discussion on the mantle structure below is highly questionable
- We recommend the authors to consider this effect in their modeling, or at least to show how the effect is observed in all the analyzed data

Abstract The significance of sediment reverberations on receiver functions of broadband OBS data is discussed. In particular, the data analyzed by Olugboji et al. recently in this journal show such effects which need to be carefully modeled. We also suggest that the LQ-coordinate rotation for the receiver function analysis should be avoided for OBS data.

1. Introduction

The significance of sediment layer (and also water layer) reverberations in seismic observation in the ocean is well recognized, and it has been one of the most challenging factors that hamper investigating deeper crustal and mantle structures [e.g., *Godin and Chapman*, 1999; *Zeldenrust and Stephen*, 2000; *Ball et al.*, 2014; *Ruan et al.*, 2014; *Bell et al.*, 2015; *Abe and Kawakatsu*, 2015; *Audet*, 2016]. *Olugboji et al.* [2016] (hereinafter OPKS16) has recently, however, reported in this journal about their receiver function analyses of OBS data without considering this effect, and discussed about the nature of the seismic LAB beneath the ocean. While such an attempt is generally a welcome one to promote OBS related research, there is some concern about how the sediment reverberations might affect their results. This is a short comment on their analyses to draw attention of potential OBS data users to consider and recognize the significant effect of the sediment layer reverberations on OBS data.

2. Significance of Sediment Reverberations on Receiver Functions of Broadband OBS Data

The OBS data used in OPKS16 are from the Stagnant Slab Project [*Fukao et al.*, 2009] in which Japanese researchers deployed broadband ocean bottom seismometers (BBOBSs) in the Philippine Sea [e.g., *Isse et al.*, 2009; *Takeo et al.*, 2013]. Figure 1 shows P-wave spectra of three component seismograms at a station T06, for which OPKS16 shows their analysis result in their Figure 5. Spectra are calculated for 200 s long seismograms that begin at 50 s before P-wave arrivals. Horizontal seismograms are rotated into radial and transverse components, and spectra are averaged for about 50 events ($M_w > 6.0$) that occurred between November 2006 and October 2007. The dominance of horizontal components (especially the radial component) can be seen. It should be also noted that horizontal component spectra show distinct peaks at ∼0.2 Hz, ∼0.4–0.5 Hz, ∼0.8 Hz, etc. that are due to reverberations of nearly-vertically traveling S-waves in the sediment layer. It is possible to constrain the structure of the sediment layer by using this information [e.g., *Godin and Chapman*, 1999; *Zeldenrust and Stephen*, 2000; *Abe and Kawakatsu*, 2015], but here we just use the frequency 0.2 Hz of the fundamental resonance to obtain a rough estimate of the S-wave speed of 240 m/s for an assumed thickness 300 m of the sediment layer (there is a trade-off between these two parameters).

Synthetic receiver functions (RFs) are calculated for such a sediment layer structure, and shown in Figure 2 (detailed characteristics of the effect of sediment reverberations to the RF analysis will be presented elsewhere [e.g., *Abe and Kawakatsu*, 2015; *Audet*, 2016]. Synthetic seismograms (with a slowness of 0.058 s/km) are calculated for a structure with a water layer (∼4600 m thick for T06) plus the sediment layer (Vp=1600 m/s, Vs=240 m/s) over a half space (Vp=8180 m/s, Vs=4720 m/s) and for a structure with an additional crust layer (Vp=6780 m/s, Vs=3660 m/s, 6 km thick) just above the half space. The extremely low Vs (i.e., high Poisson's ratio) is a general feature of marine sediment [e.g., *Hamilton*, 1971; *Shinohara et al.*, 2008]. In addition, to compare
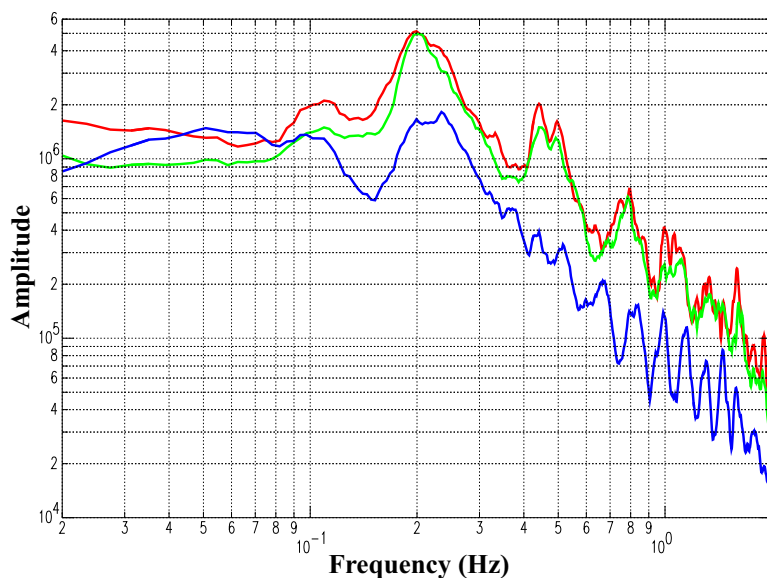
Figure 1. P-wave velocity spectra at station T06. Vertical (blue), radial (red) and transverse (green) component spectra are shown.

with a potential LAB signal, a discontinuity structure with a velocity reduction (10% in Vs) at a depth of 50 km from the sea floor is modeled. The receiver is located on the top of the sediment layer to mimic the OBS observation situation. Although individual synthetic seismograms are not presented here, reverberations in the sediment and water layers dominate radial and vertical component seismograms, respectively, even for the case with a crustal layer. This indicates that RFs obtained from radial and vertical component seismograms are also dominated by the effect of reverberations. RFs are estimated by the spectral division (radial over vertical) with a water level of 0.01 (a low-pass Gaussian filter with a parameter $\alpha = 3$ is applied to mimic OPKS16's analyses).

Obtained RFs show a consistent pattern that has a positive peak at about 1 s followed by a negative peak at about 3 s later. The initial positive peak is due to the P-to-S converted phase at the bottom of the sediment layer. Because of the extremely slow S-wave speed in the sediment, this wave travels almost vertically to cause a large motion in the horizontal component to dominate it (as also seen in Figure 1). The direct P-wave is quite weak in the horizontal component for a similar reason. As a result, the initial part of the radial component is dominated by the P-to-S converted wave and its reverberation phases. The second negative phase in RFs observed at about 3 s after the initial positive one is due to the first reverberation within the sediment layer, which will be followed by later reverberations in a similar fashion for some time to mask many possible crustal and mantle signatures; thus it is essential to model the effect of the sediment reverberation, as well as that of the water layer to discuss structure further below. Note that the "LAB signal" is hidden in the bottom figures in each plot of Figure 2 at about 6 s (and later).

The aforementioned characteristics of the sediment layer reverberation in RF waveforms can be observed in OPKS16's analyses in their Figure S2 where they show radial RFs (labeled as "without LQT rotation" on the right plot B). Here we reproduce the figure as Figure 3. (It should be also noticed that the almost all RFs shown in OPKS16 are likely to be those with the LQT rotation, even though they are labeled as "radial" (e.g., Figures 5, 7, 9, 11); the vertical-radial to LQ coordinate rotation is better to be avoided in the RF analysis of OBS records as will be discussed later separately.) In bottom right of Figure 3 squared by pink color, the largest positive peak just before 2 s and the largest negative phase 3 s later resemble the pattern that the sediment RFs predict (Figure 2). This indicates that the sediment reverberations are likely affecting the observed RFs in OPKS16. Figure 3 (left) with the LQT rotation, RFs somehow become much cleaner, and positive peaks are all located at around zero time. Considering that the LQT rotation is nothing but a coordinate rotation from Z(vertical)/R(radial) to L(P-polarization)/Q(SV-polarization), it is not obvious how the LQT rotation makes such a drastic change in RFs. For example, why the amplitude of Q-RF (left plot of A) at zero time is not close to zero as expected for the Q-component which is perpendicular to the incident P-wave
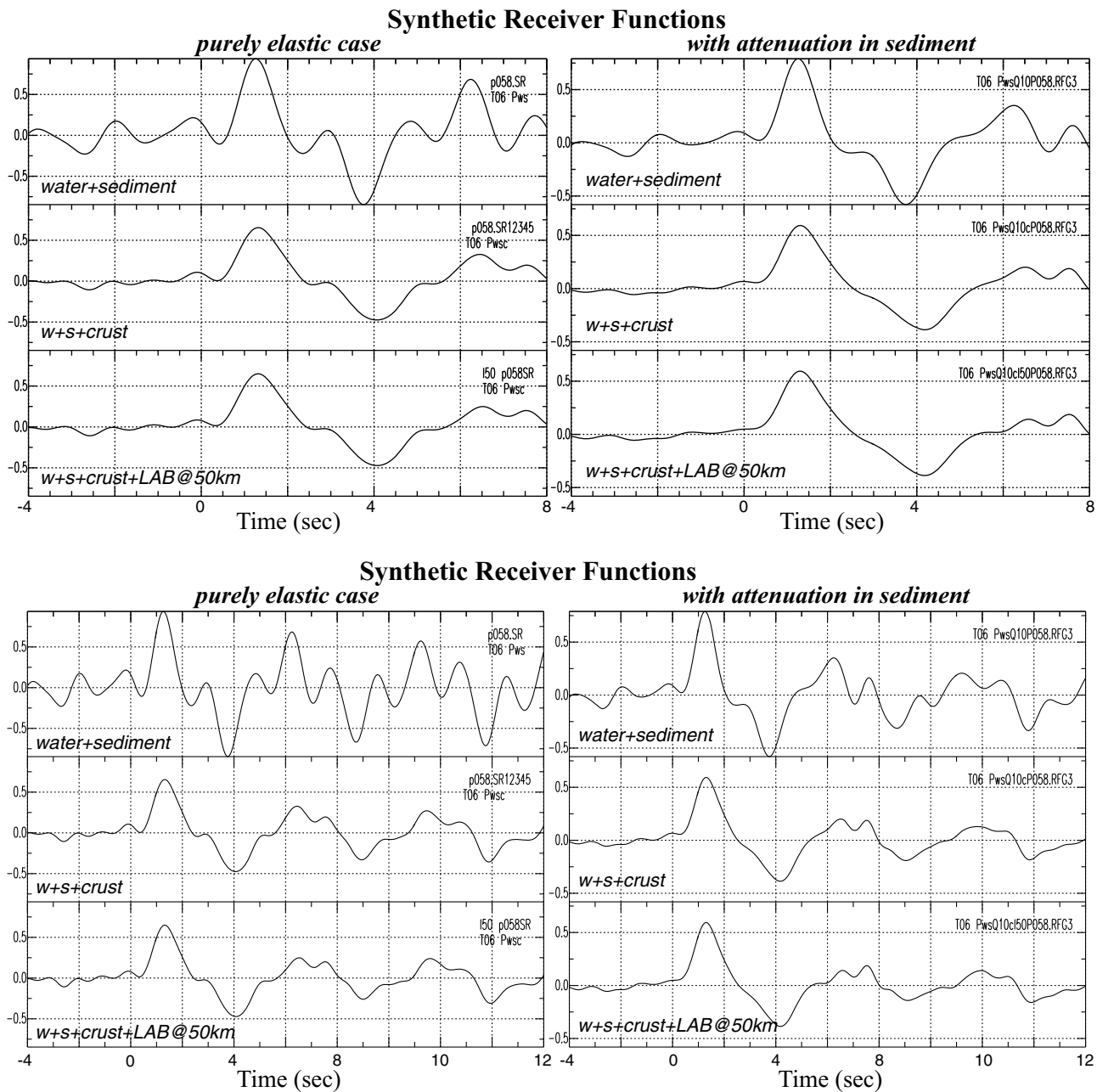
Figure 2. Two plots show the same synthetic radial RFs for station T06 (top) with water and sediment layers over a half space, (middle) with an additional crust just above the half space, and (bottom) with an additional LAB structure (a velocity reduction of 10% at 50 km from the sea floor). RFs of a purely elastic case are shown on left, and those with inelastic sediment layer ($Q_s = 10$) are shown on right. The top plot shows for a time window comparable to that of Figure 3, and the lower one for a longer time window to appreciate the reverberation effect. Note the consistent pattern of a positive phase at around 1 s, followed by a negative phase 3 s later. The exact timing of phases depends on the detail of the sediment structure, but the pattern is expected whenever there is a substantial sediment layer.

particle motion direction (i.e., L)? Also the transverse component energies (right plot of A and B), which might represent signals due to structural anisotropy, are almost completely removed after the LQT rotation, which seems rather unusual as the difference of the transverse component in two plots is whether deconvolution is done by L (in A) or Z (in B). Furthermore, the Q components show acausal energies, symmetric around the zero lag time, almost like an autocorrelation. Some explanation seems necessary. (It is also not clear how the rotation itself is conducted (what is the reference model for it? etc.).) The resulting stacked RF for the station T06 in bottom left of Figure 3, anyhow, shows a notable resemblance to those predicted by the sediment reverberation seen in Figure 2 except for a time shift. Some clarification by the authors seems
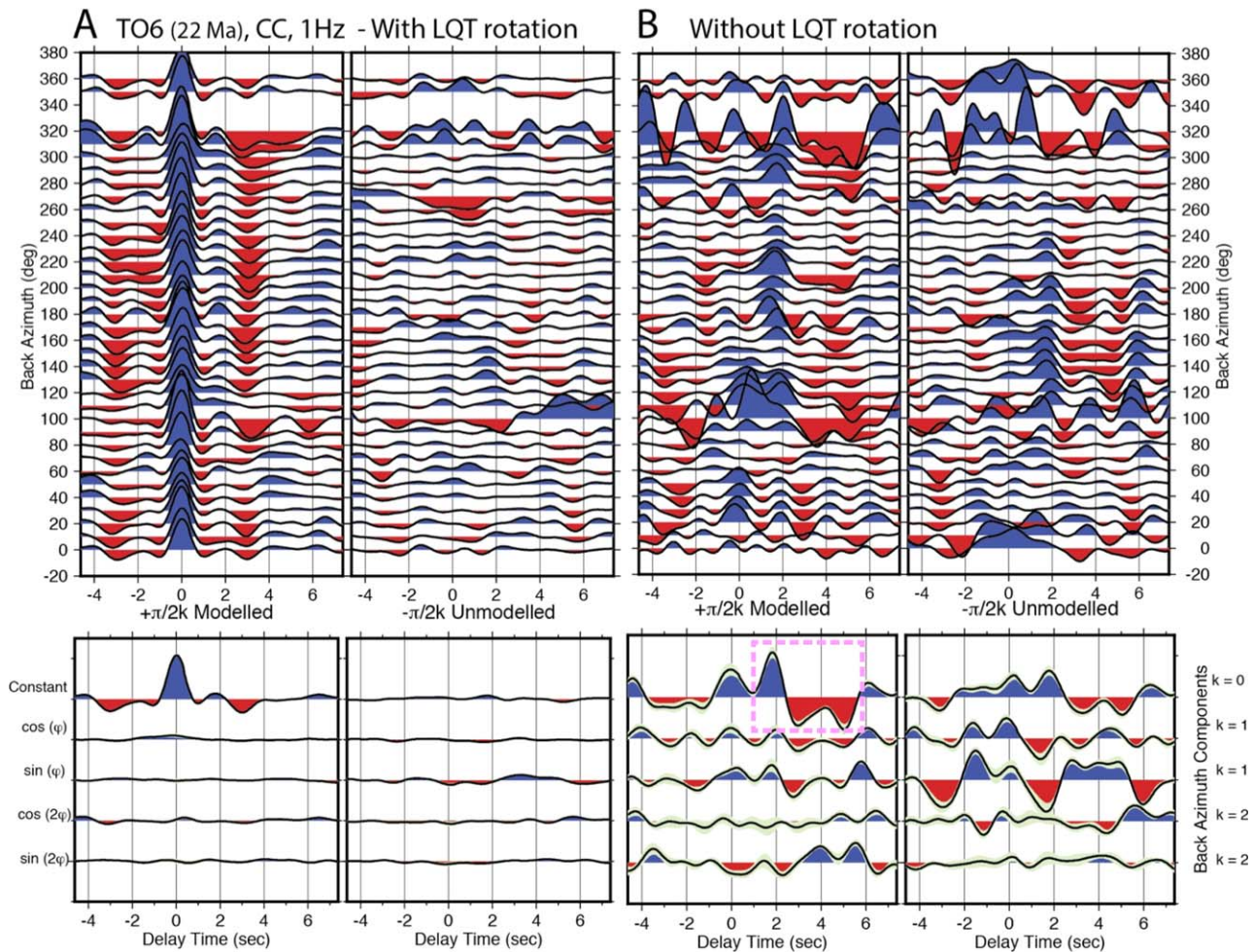
Figure 3. RFs of OPKS16 for station T06 (reproduction of their Figure S2). A box with broken pink lines indicates radial RFs that show the pattern predicted by the sediment reverberations.

to be needed. We suspect that this may not be just a coincidence and that the resultant RF may somehow reflect the effect of the sediment layer reverberations, which should not be interpreted as a signature from a deeper structure.

2.1. Comment on the Rotation From Vertical-Radial Coordinate to LQ Coordinate for OBS Data

We consider this should be avoided for P-RF analyses using OBS data [e.g., *Kumar et al.*, 2011; *Audet*, 2016]. This is because horizontal component and the vertical component records are severely affected by the signal (incoming P-wave) generated sediment-layer and water-layer reverberations, respectively. As far as we deal with them separately, there is a possibility of modeling their effects; but once we mix them together via LQ-rotation, it seems almost impossible to model them, and the deconvolution inherent of the RF analysis make it worse. Without modeling them, it seems impossible to discuss the detail of the deeper structure.

3. Comments on OPKS16

We hope that the significance of sediment layer reverberations for the RF analysis of OBS data has become clear, and their presence in the OBS data analyzed by OPKS16 is recognized. As to comments on *Olugboji et al.* [2016], we suggest that the following points should be considered seriously and further addressed by the authors.

1. The effect of sediment layer reverberations should be estimated and modeled first in the original horizontal component seismograms for each station.

2. The effect of sediment layer reverberations should be then incorporated in both RF analyses and waveform modeling. The effect not only affects the initial part of RFs but also the later part, as the reverberations are sustained, which makes modeling for deeper structure very challenging.

3. Although it is better to use the vertical-radial coordinate, if the authors prefer the LQT coordinate, figures like OPKS16's Figure S2 (Figure 3 here) should be shown for all the analyzed stations so that readers can judge the quality of RFs and the effect of sediment reverberations on RF waveforms. In this case, it seems that the authors need to explain how the LQT rotation cleans up RFs that allows them to make further interpretation. Also all the LQ-rotated RFs should be labeled so, instead of being labeled "radial" as seems to be now. Further how the rotation itself is conducted (e.g., how the angles between the vertical and L/Q directions are determined) should be described.

4. Until all above are incorporated in the analyses, further discussions on the deeper structure seem rather premature.

References

Abe, Y., and H. Kawakatsu (2015), Effects of sediment layer and shallow portion of the oceanic crust on waveforms of broadband ocean bottom seismometers in morthwest Pacific ocean, Abstract S23D-2777 presented at 2015 Fall Meeting, AGU, San Francisco, Calif., 14–18 Dec.

Audet, P. (2016), Receiver functions using OBS data: promises and limitations from numerical modelling and examples from the Cascadia Initiative, *Geophys. J. Int.*, *205*, 1740–1755, doi:10.1093/gji/ggw111.

Ball, J. S., A. F. Sheehan, J. C. Stachnik, F.-C. Lin, and J. A. Collins (2014), A joint Monte Carlo analysis of seafloor compliance, Rayleigh wave dispersion and receiver functions at ocean bottom seismic stations offshore New Zealand, *Geochem. Geophys. Geosyst.*, *15*, 5051–5068, doi:10.1002/2014GC005412.

Bell, S. W., Y. Ruan, and D. W. Forsyth (2015), Shear velocity structure of Abyssal Plain sediments in Cascadia, *Seismol. Res. Lett.*, *86*, 1247–1252, doi:10.1785/0220150101.

Fukao, Y., M. Obayashi, T. Nakakuki, and Deep slab project group (2009), Stagnant slab: A review, *Annu. Rev. Earth Planet. Sci.*, *37*, 19–46.

Godin, O. A., and D. M. F. Chapman (1999), Shear-speed gradients and ocean seismo-acoustic noise resonances, *J. Acoust. Soc. Am.*, *106*, 2367–2382.

Hamilton, E. L. (1971), Vp/Vs and Poisson's ratios in marine sediments and rocks, *J. Acoust. Soc. Am.*, *66*, 1093–1101, doi:10.1785/0220150101.

Isse, T., et al. (2009), Seismic structure of the upper mantle beneath the Philippine Sea from seafloor and land observation: implications for mantle convection and magma genesis in the Izu-Bonin-Mariana subduction zone, *Earth Planet. Sci. Lett.*, *278*, 107–119.

Kumar, P., H. Kawakatsu, M. Shinohara, T. Kanazawa, E. Araki, and K. Suyehiro (2011), P and S receiver function analysis of seafloor borehole broadband seismic data, *J. Geophys. Res.*, *116*, B12308, doi:10.1029/2011JB008506.

Olugboji, T. M., J. Park, S. Karato, and M. Shinohara (2016), Nature of the seismic lithosphere-asthenosphere boundary within normal oceanic mantle from high- resolution receiver functions, *Geochem. Geophys. Geosyst.*, *17*, 1265–1282, doi:10.1002/2015GC006214.

Ruan, Y., D. W. Forsyth, and S. W. Bel (2014), Marine sediment shear velocity structure from the ratio of displacement to pressure of Rayleigh waves at seafloor, *J. Geophys. Res. Solid Earth*, *119*, 6357–6371, doi:10.1002/2014JB011162.

Shinohara, M., T. Fukano, T. Kanazawa, E. Araki, K. Suyehiro, M. Mochizuki, K. Nakahigashi, T. Yamada, and K. Mochizuki (2008), Upper mantle and crustal seismic structure beneath the northwestern Pacific basin using a seafloor borehole broadband seismometer and ocean bottom seismometers, *Phys. Earth Planet. Inter.*, *170*, 95–106.

Takeo, A., K. Nishida, T. Isse, H. Kawakatsu, H. Shiobara, H. Sugioka, and T. Kanazawa (2013), Radially anisotropic structure beneath the Shikoku Basin from broadband surface wave analysis of ocean bottom seismometer records, *J. Geophys. Res. Solid Earth*, *118*, 2878–2892, doi:10.1002/jgrb.50219.

Zeldenrust, I., and R. A. Stephen (2000), Shear wave resonances in sediments on the deep sea floor, *Eos Trans. AGU*, *81*(48), Fall Meet. Suppl., Abstract S51B-04.